# Calculation of Threshold Displacement Energies in $UO_2$

Benjamin Reid Dacus

October 13, 2017

**Abstract**

Using Molecular Dynamics (MD) the threshold displacement energy ($E_d$) for oxygen and uranium were determined in uranium dioxide ($UO_2$) at 1500 K. Using three unique interatomic potentials, Basak, Yakub, and Yamada, all splined with a repulsive potential for close particle interactions, three different metrics were applied to determine the threshold displacement energies of particles in $UO_2$. This was accomplished through the use of a primary knock-on atom (PKA) that was given an initial energy and observed throughout the resulting cascade. By analyzing multiple PKA directions and a wide range of energies for both uranium and oxygen PKA's, curves were constructed as a function of energy investigating the following metrics: the probability of forming a stable Frenkel defect, the probability of having the PKA leave its original lattice site, the average number of displaced uranium atoms due to the PKA, and the average number of oxygen atoms displaced due to the PKA. This work provides critical insight into the varying behavior between oxygen and uranium PKA's and provides clarity regarding the various definitions of $E_d$ in a thorough manner.

# 1 Introduction

Uranium dioxide ($UO_2$), as a common nuclear fuel, has been thoroughly studied both through theoretical and experimental research methods over the majority of the last century. With the data obtained from numerous years of experiments, correlations can be developed for a range of thermo-mechanical behaviors that are coupled and input into continuum level fuel performance codes. If these fuel performance codes are provided with both the empirical correlations and the associated molecular theory, the simulations can be both descriptive and predictive of nuclear fuels like $UO_2$. This allows for the research of complex systems without the costs and safety risks involved with experimentation on nuclear materials.

Nuclear fuels undergo very high neutron flux and fluence during operation, in addition to high energy fission fragments and alpha particles released during radioactive decay of fission products. The ability to quantify the damage resulting from this radiation is a critical step in describing and understanding microstructural evolution of nuclear fuel. The threshold displacement energy ($E_d$) is a critical measure of a material's response to radiation damage because it describes if atoms will leave their lattice site, and possibly form a defect within the structure. The amount of damage that a material system experiences under irradiation is typically described in displacements per atom (dpa). Models such as the Norgett-Robinson-Torrens (NRT) [1] utilize a threshold displacement energy to calculate a given *dpa* based on the material and irradiation condition. It is thus critical to possess an accurate description of $E_d$ in order to accurately assess the number of *dpa* the material system of interest experiences.

Although $E_d$ has been studied rather in-depth in the past, there still exists some ambiguity on the definition of threshold displacement energy and how one would determine it. Meis and Chartier [2] define the threshold displacement energy as the "minimum energy transferred to a lattice atom along a given crystallographic direction yielding the creation of a stable Frenkel defect". However, other authors such as Devanathan et al. [3] define the threshold displacement energy as "the minimum energy needed to displace an atom from its lattice site." This definition is still unclear with respect to how displacement is defined. For instance, the energy required to remove atoms from a lattice site permanently is higher than the energy required to remove an atom from is lattice site and have it eventually return. A clearer expansion on that definition is described by Motta et al. where $E_d$ is "the minimum energy required to sufficiently move the atoms so that they do not return to their initial sites" [4]. It is worth investigating all three definitions of the threshold displacement energy separately in order to ascertain the differences in the hopes of implementing the correct definition for the correct application.

There have been several works over the past three decades with respect to investigating $E_d$ in $UO_2$. Early work by Soullard [5–7] determined, using electron microscopy and room temperature $UO_2$ samples, that the threshold displacement energies in $UO_2$ were 20 eV for oxygen and 40 eV for uranium and used these values to create a "computer code which makes it possible to determine the number of atoms displaced by a heavy ion slowing down in a diatomic target" [7]. Following these works, molecular dynamics simulations were used to investigate $E_d$ and the cascade effects of radiation. The research on threshold displacement energies preformed with molecular dynamics [3, 8, 9] reported similar results to Soullard with $E_d$ values for oxygen and uranium of 20 and 40 eV, respectively. Similarly, these previous computational studies utilized the definition of $E_d$ as the displacement of an atom off its lattice site. Other works, such as Meis and Chartier [2] used the sudden approximation method within the Mott-Littleton approach [10], rather than molecular dynamics, in order to determine $E_d$. They found the value of $E_d[O]$ as "approximately" 20 eV, and $E_d[U]$ as "rather close to" 50 eV. Meis and Chartier's higher ura-

nium $E_d$ value, defining $E_d$ as the energy at which stable defects are formed, is likely higher than other works due to the fact that higher energy particles would be needed to create a defect rather than to just leave their lattice site.

With common MD simulations, threshold displacement energies are typically observed through the movement of a primary knock-on atom (PKA) due to a supplied initial energy and the eventual interaction of the PKA with other atoms in a lattice. Determination of $E_d$ for uranium and oxygen in $UO_2$ is useful for the studies of high energy PKA's [8, 9, 11] and the cascade simulations that can be performed. Using repulsive potentials splined with typical pair potentials and the implementations of PKA's in simulations, authors such as Martin et al. [11] created curves of defect formation and fit to the NRT law so as to extrapolate the threshold displacement energies of particular materials like $UO_2$.

By systematically increasing the PKA energy over a prescribed range of energies, a curve illustrating the probability of Frenkel pair formation as a function of PKA energy can be generated. In a system at 0 K, this probability distribution would be a step function. However in a system with higher temperatures, the thermal fluctuations smooth out this step function and create a continuous curve. The shapes of the probability curves created show the effects on $E_d$ due to thermal fluctuations that exist in a system at 1500 K. This temperature was selected as the system temperature as this is a common operating nuclear fuel temperature. For a simulation run at 0 K, there would be a single quantity of $E_d$ and a step function of defect and PKA displacement probabilities due to the lack of particle vibrations. Therefore, the simulations in our work that were run at 1500 K and contain thermal fluctuations, provide smooth probability curves that explain the properties of a nuclear fuel at a realistic operating temperature. Furthermore, no high temperature investigations of $E_d$ in $UO_2$ have been previously performed to create probability functions of threshold displacement energy.

In this study we will determine the threshold displacement energies for uranium and oxygen in $UO_2$ at 1500 K. The threshold displacement energy is investigated through the following metrics: if the PKA left the lattice site at any time; if the PKA led to the creation of a stable Frenkel defect; and the number of displaced atoms following the immediate return to a thermal state after PKA introduction. A further expansion on the previous, and rather ambiguous, definition of $E_d$ will show the calculated threshold displacement energy as a function of particle type, and the initial direction of the PKA. This will be performed utilizing PKA's from both species and examining the effect of each species PKA on each sublattice. The simulations will also be carried out with the use of three unique potentials that will be discussed later. These different metrics will create a thorough model of the threshold displacement energies for uranium and oxygen in $UO_2$, expanding on all previous definitions of the property.

# 2 Potentials

A standard molecular dynamics (MD) simulation consists of a collection of particles, a potential energy function that defines the ways in which the particles interact, and a given time frame in which the equations of motion are used to update the state of the system. In this study, molecular dynamics was used to determine the threshold displacement energies rather than other methods like density functional theory (DFT) because it is computationally inexpensive by comparison and it still yields accurate results. The use of the Nose-Hoover [12] thermostat within the MD simulation allows the temperature to be brought to a certain point and maintained. In our study we used this method within the LAMMPS [12] code in order to determine the threshold displacement energies.

The interatomic potential used to govern particle interactions is the most fundamental aspect of any MD simulation. The atomic potential is designed in such a way that it should account for the coulombic, nuclear and any other forces

that occur within the system of particles. Of the many potentials that exist for modeling $UO_2$, the three that were used in the present study include: Basak, Yamada, and Yakub [13–15]. Previous works [16–18] show that all three of these potentials exhibit capabilities to reproduce close to experimental results when tested at temperatures and pressures that were not extremely high. The Yamada and Yakub potentials were selected specifically because of their close approximations of physical properties of $UO_2$ at 1500 K such as the lattice parameter $a_0$, specific heat $c_p$, and the Bulk modulus $K$ [17]. The Basak potential was selected because it is an improved fitting of the Yamada potential, created by using isothermal compressibility data in order to better model the lattice parameter and lattice expansion [13].

The potentials used in this study do not, however, contain a repulsive potential in their original state sufficient to model small distance interactions between atoms. For this reason, the widely known Ziegler-Biersack-Littmark (ZBL) [19] potential was splined to the three separate potentials so that high energy atoms would interact with other atoms in a more physical manner. This ZBL spline occurred between 0.35 and 1.34 Angstroms for the O-O interaction, 1.7 and 2.12 Angstroms for the U-U interaction, and 0.64 and 1.09 Angstroms for the U-O interaction.

# 3 Computational Details

In order to determine $E_d$, we need to induce a mini-cascade via the addition of extra kinetic energy to the PKA. This PKA and all other atoms are monitored so that the three threshold displacement energy metrics can be profiled. These metrics include the measurement of: the maximum PKA displacement from its original coordinates (did it leave its lattice site), the formation of a stable Frenkel defect, and the number of displaced atoms (on both the oxygen and uranium sublattices). The displacement data was a comparison of atom coordinates at different times, while the defect calculations were found by implementing the Voronoi package within the LAMMPS code [12, 20].

Simulations were run at low PKA energies in the 5-65 eV range and higher energies in the 150-200 eV range in order to fully investigate the breadth of atomic displacements in the system. The simulations at low energies (5 to 65 eV) consisted of 6144 particles and ran for a total time of 5.5 picoseconds following the introduction of the PKA and an equilibration time of 2.5 picoseconds. The higher energy runs (150 to 200 eV) for oxygen atoms were run with 32,928 atoms so that they had an equivalent energy per atom ratio to the lower energy runs. The high energy runs required longer times to equilibrate (5 picoseconds), so although the total run time was also 5.5 picoseconds following the introduction of the PKA, the equilibration time was much longer than the low energy runs. All of the runs were split up into categories depending on the different simulation modifications to the PKA, such as the initial direction of travel, the energy supplied to the particle, the particle type of the PKA (Uranium or Oxygen), and the potential used to define the particle interactions. Each subgroup of the different combinations of categories was run with 40 independent runs where unique initial velocities were assigned to all particles with the exception of the PKA. The energies tested for the uranium PKA's were in increments of 5 eV from 5 to 65 eV. This energy range was chosen because the previous $E_d$ findings for uranium showed the highest value of $E_d$ at 50 eV. For the oxygen PKA's, the energies were also incremented by 5 eV but from 5 to 40 eV because this encompasses the $E_d$ previously found in other works. The oxygen PKA's were also simulated from 150 to 200 eV in increments of 10 eV in order to show the displacement of uranium atoms due to oxygen PKA's. Furthermore, all PKA's were tested in the following directions: [110], [130], [141], [214], [232], and [313]. These directions were selected because they offer a range of both low and high symmetry directions. With all of these variables included, there was a total of 6480 runs for each of the three potentials,

allowing for 19,440 total runs.

The simulation process (following the initialization of the structure) was carried out as follows: First, minimize the structure. Then, equilibrate the system in an NPT ensemble at 1500 K and 0 bars for 2.5 picoseconds (5.0 picoseconds for high energy runs) using the Nose-Hoover thermostat and barostat. After this is completed, initialize the PKA's velocity and direction and run in an NVE ensemble for 5.5 picoseconds. Then, drop the temperature of the system with two separate quench runs for 10.0 and 3.75 picoseconds, respectively. The two quench runs exist so that the system does not minimize to a metastable state, where both quench runs decrease the temperature a specified amount. Lastly, minimize the structure again and output positions so that the positions of the particles can be directly compared to the originally minimized structure.

Atomic positions were output at various times throughout the simulation in order to accurately investigate the threshold displacement energy using all three discussed metrics. Following each individual output of atomic positions, the system was quenched down to 0 K for direct comparison to a minimized structure in order to avoid noise from thermal motion. In order to directly compute the number of atom displacements without the effects of interstitial diffusion increasing the number of displaced atoms, the system was immediately quenched down to 0 K following the return to a thermal state after the cascade. However, the simulation needed to run for a much longer time after it reached thermal equilibrium in order to determine whether defects that were formed during the cascade remain after the rapid annihilation of Frenkel pairs. For this reason, two separate post-processing output points are used; one that allows for several picoseconds to pass after the dissipation of the thermal spike, and one immediately following the dissipation of the thermal spike.

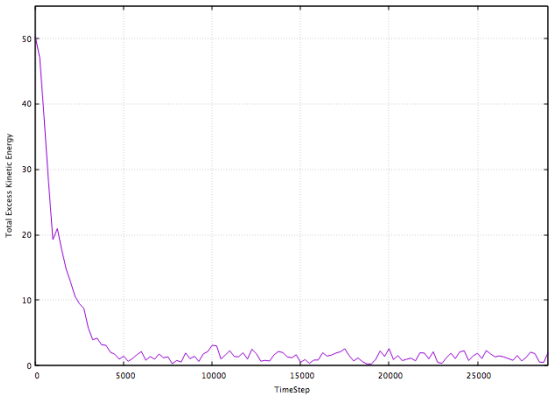


Figure 1: Total Excess kinetic energy for all atoms above 1 eV versus time following the introduction of the PKA.

Analysis of this simulation determines the time at which the structure returned to a thermal state (suggesting the thermal spike has dissipated). The specification for the determination of a thermal state was when the sum of excess kinetic energy, $\sum(KE-1eV)$, of all atoms above 1 eV was less than 5 eV. The high energy runs, because there were more atoms, had a cutoff energy of 25 eV rather than 5 eV. These specifications were chosen because they are sufficiently strict to ensure that the PKA energy spike has dissipated. Figure 1 shows the total excess kinetic energy of atoms above 1 eV over time following the introduction of the PKA. The thermal state is reached around time step 3,500 where the sum of excess kinetic energy of all particles above 1 eV was equal to 5 eV. The figure is made from an arbitrary run in which the PKA was a uranium atom at 50 eV, hence the initial energy of approximately 50 eV.

The calculation of atom displacements immediately following the thermal spike was implemented due to both the self-healing mechanism of oxygen interstitials in a string-like fashion and the rapid diffusion of oxygen interstitials over time in the structure [21]. If the displacement of atoms was calculated from the initial run with a large equilibration time following the PKA, there would have been a significant number of outliers

in the number of displaced atoms among runs due to these two effects. Quenching immediately after the system reaches thermal equilibrium serves to calculate the number of displaced atoms, without the added statistical noise that would be induced by diffusion or oxygen self-healing.

# 4 Results and discussion

## 4.1 Frenkel Pair Formation Probability Curves

Figure 2 shows the Frenkel pair formation probability as a function of PKA energy for simulations that were run with both uranium and oxygen PKA's for six unique directions. The oxygen data does not offer results in which clear directional dependence can be seen because the oxygen PKA's had a significantly smaller probability of forming defects at any given energy when compared to the uranium results. These directional contributions for oxygen will be seen with higher energy PKA's, however when the PKA is tested around the experimentally reported TDE value (20 eV), it is not clearly defined.

There is a clear directional dependence in the uranium PKA probability curves. The [214] direction consistently showed the lowest probabilities for defect formation across all three potentials. Although [110], [130], [141], and [232] gave very close probabilities of defect formation at the 65 eV energy for uranium results, directions [130] and [141] had higher energy averaged probabilities than all other directions showing that those directions give the highest probabilities of forming a defect at any energy. Overall, there is good agreement among the potentials considering the directional dependencies and range of probabilities of defect formations.

Given the definition of $E_d$ as the lowest energy at which defect formation occurs, then $E_d$ for oxygen ($E_d[O]$) is 20 eV for the Basak results and 30 eV for both the Yakub and Yamada results by the lowest seen energy of defect formation in figures 2a-c. Similarly, by this same definition, the uranium TDE, $E_d[U]$ is 30 eV for the Basak and Yakub potentials, and 25 eV for the Yamada potential as seen in figures 2d-f. However, these values are only applicable for specific directions. Therefore the angularly averaged value of $E_d[O]$ and $E_d[U]$ are higher and involve averaging over a wide range of directions. A crystallographically averaged $E_d$ with respect to a PKA leading to the formation of a Frenkel pair can be determined by averaging over all directions at the point where each direction's probability curve reaches 50 %. This generates a crystallographically average quantity that describes when it is probable that a PKA will lead to the formation of a Frenkel defect. This is not applicable for oxygen data because the oxygen TDE spectra do not reach 50 % due to the tendency of oxygen defects to rapidly annihilate. This 50 % averaged mark being considered and assuming that the six directions are adequate in finding a representative average, the value of $E_d[U]$ is 54 eV for Basak, 54 eV for Yakub, and 55.5 eV for Yamada.

## 4.2 Lattice Site Displacement Probability Curves

Figure 3 shows the probability that an oxygen or uranium PKA will leave its lattice site for a given energy and direction. For the oxygen probability curves, the lowest energy $E_d[O]$ is 5 eV in the [130] direction seen in figure 3a. Similarly, the lowest energy $E_d[U]$ at which a uranium atom leaves its lattice site is 15 eV seen in figures 3d-f.

A crystallographically averaged $E_d$ with respect to an atom being displaced from its lattice site can be determined by averaging over all directions at the point where each direction's probability curve reaches 50 %. This generates a crystallographically average quantity that describes when it is probable that an atom will leave its lattice site. Assuming that the six directions are adequate in finding a representative average, $E_d[O]$ is 17 eV, and $E_d[U]$ is 30 eV. These values of $E_d$

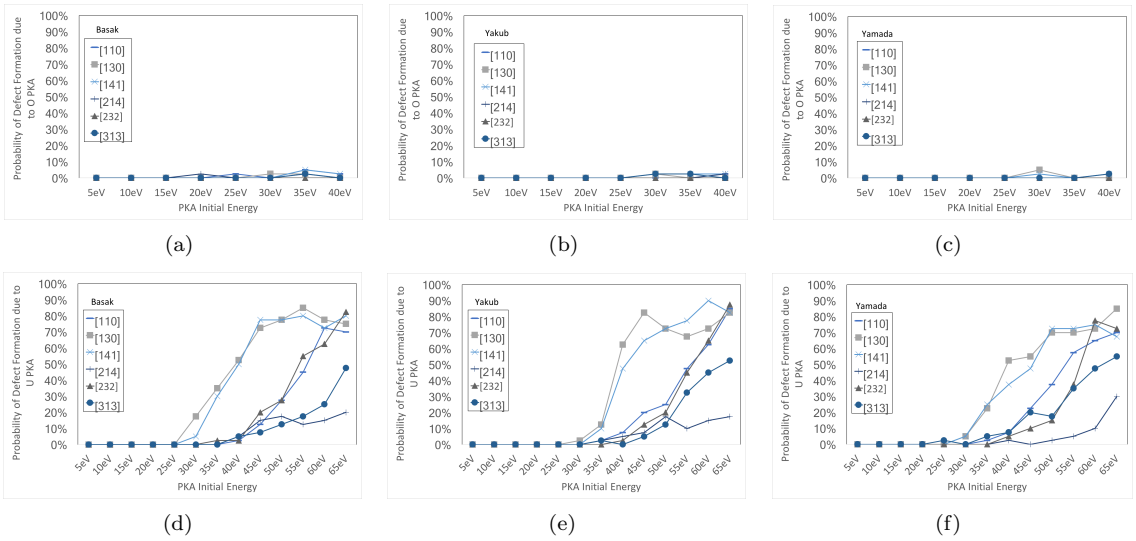


Figure 2: Defect Formation Probability as a function of PKA energy in $UO_2$ due to Uranium and Oxygen PKA's in directions [110], [130], [141], [214], [232], and [313]. Left to Right Figures: Basak (a,d), Yakub (b,e), Yamada (c,f). Top row (a-c) is defects formed by oxygen PKA's, bottom row (d-f) is defects formed by uranium PKA's.

are lower than previous results [2, 5, 6] and this is likely due to the way in which the previous works defined the TDE.

Oxygen PKA's show a large directional dependence but the nature of the dependence is not consistent across the three potentials. This is due to the difference in oxygen sublattice properties over potentials, such as the improvement in the lattice parameter of the Basak potential compared to the Yamada potential [13]. The uranium plots are extremely consistent across the three potentials and this shows that the uranium sublattice has consistent properties between different interatomic potentials.

Between the different PKA's probability curves, the highest symmetry direction [110] displays very different behavior. Figures 3a-c show that the oxygen PKA's moving in the [110] direction are consistently displaced more than any other direction. This is the opposite of what is seen for the uranium PKA's in figures 3d-f, where uranium PKA's moving in the [110] direction are consistently displaced less than any other direction.

## 4.3 Displaced Oxygen Atoms due to PKA

Figure 4 shows the average number of permanently displaced oxygen atoms due to the uranium and oxygen PKA's in all directions for all potentials. There is a significant difference between the potentials, in that comparably very high numbers of oxygen atoms are displaced by the uranium PKA in the simulations that utilized the Yamada interatomic potential, seen in figure 4c. Using the Yamada potential, the average number of displaced oxygen reaches a maximum of 12, while the other potentials displaced at most 6 oxygen atoms. This is due to the oxygen sublattice properties defined by the Yamada potential. Because the Basak potential is considered an improvement of the Yamada potential, and its results agree with the Yakub potential, the Yamada is not seen as producing the most accurate oxygen sublattice behavior. Although

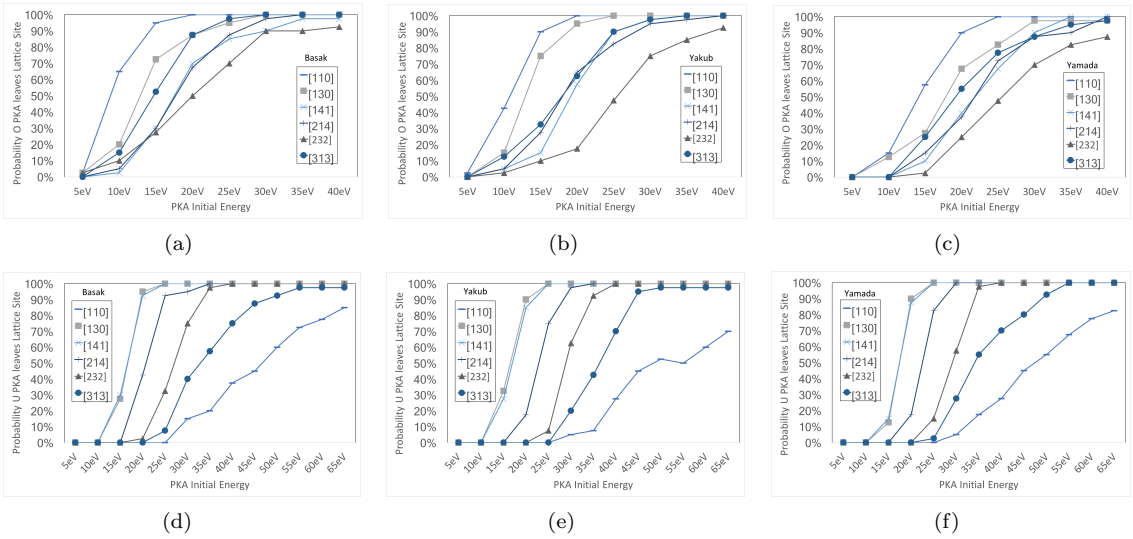


Figure 3: Probability that PKA leaves lattice site as a function of PKA energy in $UO_2$ due to Uranium and Oxygen PKA's in directions [110], [130], [141], [214], [232], and [313]. Left to Right Figures: Basak (a,d), Yakub (b,e), Yamada (c,f). Top row (a-c) is PKA displacements of oxygen PKA's, bottom row (d-f) is PKA displacements of uranium PKA's.

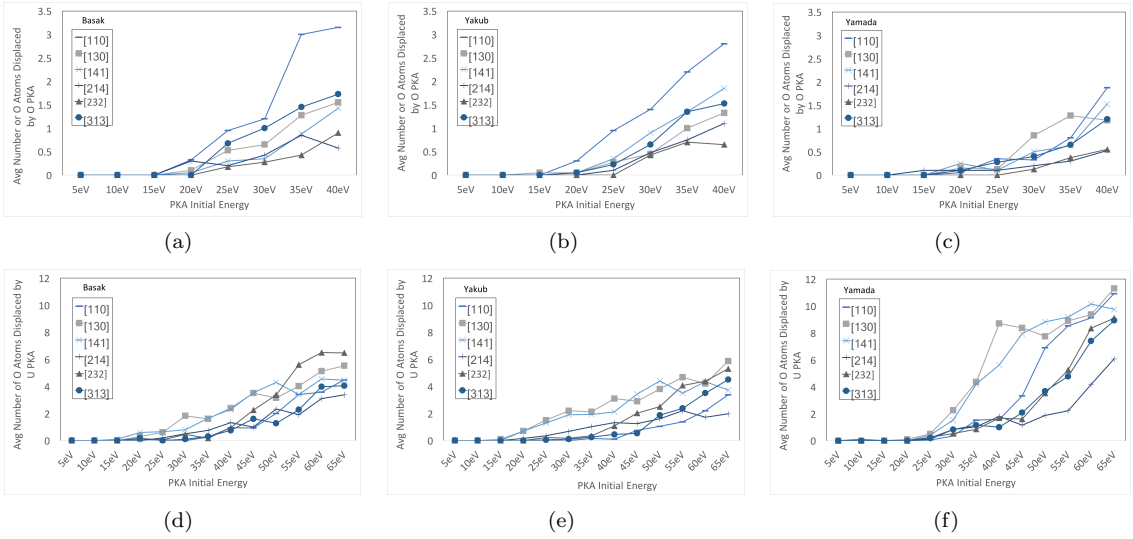


Figure 4: Average number of oxygen atoms displaced by a PKA as a function of PKA energy in directions [110], [130], [141], [214], [232], and [313]. Left to Right Figures: Basak (a,d), Yakub (b,e), Yamada (c,f). Top row (a-c) is displaced oxygen atoms due to oxygen PKA's, bottom row (d-f) is displaced oxygen atoms due to uranium PKA's.

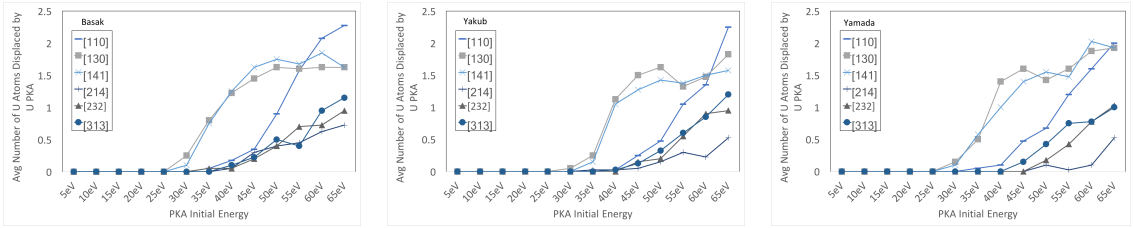


(a) (b) (c)

Figure 5: Average number of uranium atoms displaced by a PKA as a function of PKA energy in directions [110], [130], [141], [214], [232], and [313]. Left to Right Figures: Basak (a), Yakub (b), Yamada (c).

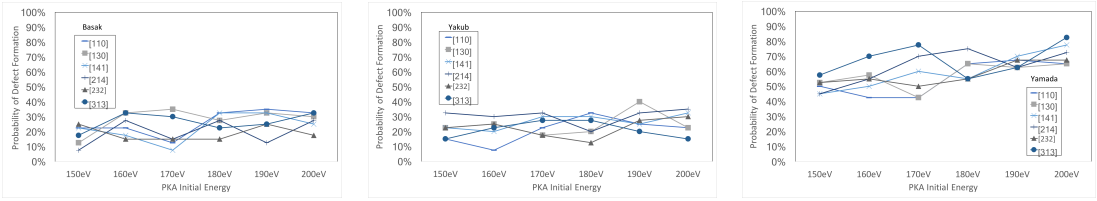


(a) (b) (c)

Figure 6: Defect Formation Probability due to High Energy O PKA as a function of PKA energy in directions [110], [130], [141], [214], [232], and [313]. Left to Right Figures: Basak (a), Yakub (b), Yamada (c).

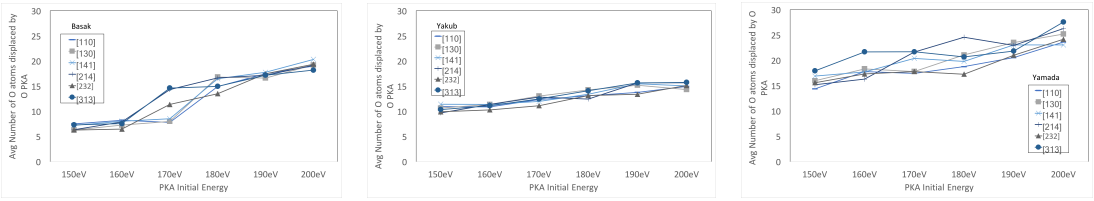


(a) (b) (c)

Figure 7: Average number of oxygen atoms displaced by High Energy O PKA as a function of PKA energy in directions [110], [130], [141], [214], [232], and [313]. Left to Right Figures: Basak (a), Yakub (b), Yamada (c).

the Yamada potential exhibits properties of a more fluid oxygen sublattice when the uranium PKA is introduced, the opposite is seen with the oxygen PKA, seen in figure 4f. The Yamada potential leads to less displaced oxygen atoms than the other two potentials where the maximum number of oxygen atoms displaced by the oxygen PKA is 2 atoms for the Yamada potential but 3 for the others. Although this discrepancy is not enough to be statistically significant, it is worth noting the difference in sublattice properties over different potentials.

At the point of the experimentally found TDE for uranium, 40 eV [5–7], the average number of displaced atoms by the uranium PKA at 40 eV was 1.8 atoms by the Basak potential, 1.9 atoms by the Yakub potential, and 3.7 atoms by the Yamada potential. Thus, a single uranium PKA of 40 eV is expected to produce on average 1.8 oxygen displacements, according to the Basak potential and assuming that the six directions are adequate in finding a representative average. The maximum number of permanently displaced oxygen atoms by a uranium PKA is 2.4 atoms for the Basak potential, 3.1 for the Yakub potential, and 8.7 for the Yamada potential, all in the [130] direction. The minimum number of oxygen atoms displaced by the 40 eV uranium PKA in a direction was 0.75 for the Basak potential in the [313] direction, 0.1 for the Yakub potential in the [110] direction, and 1.0 for the Yamada potential in the [313] direction.

At the point of the experimentally found TDE for oxygen, 20 eV [5–7], the average number of displaced oxygen atoms by the oxygen PKA at 20 eV is 0.15 atoms for the Basak potential, 0.15 atoms for the Yakub potential, and 0.12 atoms for the Yamada potential. Thus, for approximately every 6.7 oxygen PKA's of 20 eV, on average a single oxygen atom is displaced according to the Basak potential. The maximum number of permanently displaced oxygen atoms due to the oxygen PKA was 0.3 atoms for the Basak potential in the [110] direction, 0.3 atoms for the Yakub potential in the [110] direction, and 0.3 atoms for the Yamada potential in the [141] direction. The minimum number of displaced oxygen atoms by the oxygen PKA at 20 eV is 0 atoms for all potentials (occurred for multiple directions).

## 4.4 Displaced Uranium Atoms due to a Uranium PKA

Figure 5 shows the average number of permanently displaced uranium atoms due to the uranium PKA. The plots of the average number of displaced uranium atoms due to the oxygen PKA are not included because the values were zero for the entire low energy range. This is because the maximum energy transfer from an oxygen atom to a uranium atom is not sufficient to displace the uranium in this range.

The data obtained from the uranium PKA simulations is in relatively strong agreement across potentials and shows that a maximum number of almost 2.3 atoms were displaced when the 65 eV, [110] PKA simulations/systems reached thermal equilibrium. Averaging the directional curves at 65 eV produces 1.25 uranium atoms displaced. This is not a significant number of uranium atoms, however because the uranium PKA's need to supply enough energy to remove other uranium atoms from their lattice site, it was not expected that there would be a large number of uranium displacements. The same results are seen over all potentials and the curves are in agreement with the exception that they do not have the same exact shapes. However, the directional curves are all in the same order concerning number of uranium displacements between potentials, showing strong agreement between potentials.

At the point of the experimentally found TDE for uranium, 40 eV [5–7], the average number of displaced atoms by the uranium PKA at 40 eV was 0.5 atoms by the Basak potential, 0.65 atoms by the Yakub potential, and 0.7 atoms by the Yamada potential. Thus, for approximately every 2 uranium PKA's of 40 eV, on average a single uranium atom is displaced according to the Basak potential. The maximum number of

permanently displaced uranium atoms by the 40 eV uranium PKA is 1.2 atoms by the Basak potential in the [141] direction, 1.1 by the Yakub potential in the [130] direction, and 1.4 by the Yamada potential in the [130] direction. The minimum number of uranium atoms displaced by the 40 eV uranium PKA in a direction was 0.05 for the Basak potential in the [232] direction, and 0 for both the Yakub and Yamada potentials in the [232] direction.

### 4.5 High Energy Oxygen PKA simulations

In order to investigate the displacement of uranium atoms from an oxygen PKA, high energy oxygen PKA cascade simulations were performed. The same data that was collected for the low energy oxygen PKA simulations was collected for the high energy runs, however the displacements of atoms that interacted with the PKA and the defect formations are the only metrics of interest in the high energy runs because the PKA energy is well above the TDE value for oxygen.

Figure 6 shows the defect formation probabilities due to the high energy oxygen PKA. The curves are relatively constant and show that there is not a huge change in defect formation probability with change in energy within the energy range in figure 6. Although the Basak and Yakub potentials display similar results with respect to average directional values at each energy, the Yamada potential gives nearly double what the probability of forming a defect was for the other two interatomic potentials. This is likely due to the difference in oxygen sublattice properties that was seen in figure 4, where the oxygen sublattice is more soft than in the other simulations which use different interatomic potentials. Furthermore, there is relatively low variability over the different directions and it is also seen that there is agreement within statistical error over potentials with respect to directional dependencies.

| | [214] | [232] | [313] |
|---|---|---|---|
| 150 | 0<br>**0**<br>*0* | 0<br>**0.075**<br>*0* | 0<br>**0**<br>*0* |
| 160 | 0<br>**0**<br>*0* | 0<br>**0**<br>*0* | 0<br>**0**<br>*0* |
| 170 | 0<br>**0**<br>*0* | 0.05<br>**0.025**<br>*0* | 0<br>**0.1**<br>*0* |
| 180 | 0<br>**0**<br>*0* | 0.05<br>**0**<br>*0* | 0<br>**0.05**<br>*0* |
| 190 | 0.05<br>**0**<br>*0* | 0.175<br>**0.025**<br>*0* | 0<br>**0.1**<br>*0* |
| 200 | 0<br>**0.05**<br>*0* | 0.15<br>**0.025**<br>*0.05* | 0<br>**0**<br>*0* |

Table 1: Average Number of Displaced Uranium Atoms by High Energy Oxygen PKA as a function of PKA energy and direction. Basak, **Yakub**, and *Yamada*.

Table 1 shows the average number of displaced uranium atoms due to the high energy oxygen PKA. There is no uranium atom displacement data for the directions [110], [130], and [141]. This is because all of the values are zero due to the fact that the direction of the PKA does not allow the PKA to transfer a significant amount of energy to other particles, specifically the uranium atoms. Because the energy range that the oxygen PKA was tested with encompasses the minimum energy needed to transfer approximately 50 eV to the uranium atoms (with a direct collision), the number of uranium atoms displaced is very small. 50 eV was used because it was the largest previously reported TDE value for uranium by Meis and Chartier [2]. For an individual simulation, at most one uranium atom can be displaced, because the highest energy of the oxygen PKA in the simulations does not exceed double the energy that is needed to displace a uranium atom. In addition to the very low

number of uranium atoms displaced, the range of displacements shows gaps and inconsistent energy dependencies. This is due to statistical fluctuations where uranium displacements have low probabilities. Although there is not strong evidence to show agreement between the three potentials, none display displacements in the [110], [130], and [141] directions, and all display some results in the [232] direction. The Yakub potential shows uranium displacements in the [214], [232], and [313] directions, while the Basak potential shows uranium displacements in the [214] and [232] directions. The Yamada potential only shows uranium displacements in the [232] direction, which shows that it has a system which is least likely to show uranium displacements.

Figure 7 shows the displaced oxygen atoms due to the high energy oxygen PKA. Each plot shows a dependence on energy, however the trends are not consistent over potentials. The Yakub for instance, show very little variability over directions. This is not the case for the Yamada and in the intermediate energy range for the Basak. Furthermore, the Yamada potential gives higher numbers of displaced atoms, which is understandable due to the similar results seen in figure 4c, where the uranium PKA displaced more oxygen atoms.

In the middle of the energy range there is the most variability among potentials so the average, maximum, and minimum number of displaced atoms at 180 eV are useful to see numerically. The average number of displaced atoms by the oxygen PKA at 180 eV was 15.0 atoms by the Basak potential, 13.4 atoms by the Yakub potential, and 20.7 atoms by the Yamada potential. The maximum number of displaced oxygen atoms by the 180 eV oxygen PKA is 16.8 atoms by the Basak potential in the [130] direction, 14.3 by the Yakub potential in the [130] direction, and 24.6 by the Yamada potential in the [214] direction. The minimum number of oxygen atoms displaced by the 180 eV oxygen PKA was 13.5 for the Basak potential in the [232] direction, 12.5 for the Yakub potential in the [214] direction, and 17.3 for the Yamada potential in the [232] direction.

# 5 Conclusion

Molecular dynamics simulations of $UO_2$ using low energy PKA's have revealed the threshold displacement energy probability curves that exist for varying definitions of $E_d$. The metrics that were used include: if the PKA led to the formation of a stable Frenkel defect; if the PKA left the lattice site; and an analysis on the number of atoms that were displaced by the PKA immediately following the return to a thermal state.

Using the $E_d$ definition of the minimum energy PKA required to form a stable Frenkel defect, and assuming that this occurs at the minimum for any direction or potential, $E_d[O]$ is 20 eV according to the Basak potential and $E_d[U]$ is 25 eV for the Yamada potential. Using the point where the probability of forming a defect reaches 50 %, and assuming that the directions tested are adequate in finding a representative average for the uranium PKA, the value of $E_d[U]$ becomes 54 eV for the Basak potential.

Using the $E_d$ definition of whether or not the PKA left the lattice site and determining $E_d$ at the 50 % probability mark for each PKA probability spectra, $E_d[O]$ is 17 eV and $E_d[U]$ is 30 eV. These values would be higher if the probability spectra were found by the determination of permanently displaced PKA's. However, the spectra took into account if atoms left their lattice site at any point during the simulation so the $E_d$ values are lower than previously reported values.

The displacement of atoms during the PKA induced cascades showed that there are consistent results across the potentials Basak and Yakub. In several instances such as the displaced oxygen atoms due to the uranium PKA and the probability of defect formation at high oxygen PKA energies (figures 4 and 6), the Yamada potential displayed noticeable differences in the oxygen sublattice properties. This led to the conclusion that the Yakub and Basak potentials were more

accurate in determining the values of $E_d$ and the cascade data.

# References


[1] M. Norgett, M. Robinson, and I. Torrens, "A proposed method of calculating displacement dose rates," *Nuclear Engineering and Design*, vol. 33, no. 1, pp. 50 – 54, 1975.

[2] C. Meis and A. Chartier, "Calculation of the threshold displacement energies in uo2 using ionic potentials," *Journal of Nuclear Materials*, vol. 341, no. 1, pp. 25 – 30, 2005.

[3] R. Devanathan, T. D. de la Rubia, and W. Weber, "Displacement threshold energies in -sic," *Journal of Nuclear Materials*, vol. 253, no. 1, pp. 47 – 52, 1998.

[4] A. T. Motta, D. R. Olander, and B. Wirth, *Light water reactor materials*. American Nuclear Society, 2017.

[5] J. Soullard and E. A. Alamo, "Etude du ralentissement des ions dans une cible diatomique," *Radiation Effects*, vol. 38, no. 3-4, pp. 133–139, 1978.

[6] J. Soullard, "High voltage electron microscope observations of uo2," *Journal of Nuclear Materials*, vol. 135, no. 2, pp. 190 – 196, 1985.

[7] J. Soullard, "Contribution to the study of structural defects in uranium dioxyde," 1977.

[8] L. V. Brutzel, J.-M. Delaye, D. Ghaleb, and M. Rarivomanantsoa, "Molecular dynamics studies of displacement cascades in the uranium dioxide matrix," *Philosophical Magazine*, vol. 83, no. 36, pp. 4083–4101, 2003.

[9] N.-D. Morelon, D. Ghaleb, J.-M. Delaye, and L. V. Brutzel, "A new empirical potential for simulating the formation of defects and their mobility in uranium dioxide," *Philosophical Magazine*, vol. 83, no. 13, pp. 1533–1555, 2003.

[10] N. F. Mott and M. J. Littleton, "Conduction in polar crystals. i. electrolytic conduction in solid salts," *Trans. Faraday Soc.*, vol. 34, pp. 485–499, 1938.

[11] G. Martin, P. Garcia, L. V. Brutzel, B. Dorado, and S. Maillard, "Effect of the cascade energy on defect production in uranium dioxide," *Nuclear Instruments and Methods in Physics Research Section B: Beam Interactions with Materials and Atoms*, vol. 269, no. 14, pp. 1727 – 1730, 2011. Computer Simulations of Radiation Effects in Solids.

[12] S. J. Plimpton, "Fast parallel algorithms for short-range molecular dynamics," *J Comp Phys*, vol. 117, no. 1, pp. 1–19, 1995.

[13] C. Basak, A. Sengupta, and H. Kamath, "Classical molecular dynamics simulation of uo2 to predict thermophysical properties," *Journal of Alloys and Compounds*, vol. 360, no. 1, pp. 210 – 216, 2003.

[14] K. Yamada, K. Kurosaki, M. Uno, and S. Yamanaka, "Evaluation of thermal properties of uranium dioxide by molecular dynamics," *Journal of Alloys and Compounds*, vol. 307, no. 1, pp. 10 – 16, 2000.

[15] E. Yakub, C. Ronchi, and D. Staicu, "Computer simulation of defects formation and equilibrium in non-stoichiometric uranium dioxide," *Journal of Nuclear Materials*, vol. 389, no. 1, pp. 119 – 126, 2009. Thermochemistry and Thermophysics of Nuclear Materials.

[16] K. Govers, S. Lemehov, M. Hou, and M. Verwerft, "Comparison of interatomic potentials for uo2. part i: Static calculations," *Journal of Nuclear Materials*, vol. 366, no. 1, pp. 161 – 177, 2007.

[17] K. Govers, S. Lemehov, M. Hou, and M. Verwerft, "Comparison of interatomic

potentials for uo2," *Journal of Nuclear Materials*, vol. 376, no. 1, pp. 66 – 77, 2008.

[18] S. I. Potashnikov, A. S. Boyarchenkov, K. A. Nekrasov, and A. Y. Kupryazhkin, "High-precision molecular dynamics simulation of uo2-puo2: pair potentials comparison in uo2," *Journal of Nuclear Materials*, 2011.

[19] J. P. B. J.F. Ziegler and U. Littmark, "The stopping and range of ions in matter," *Journal of Nuclear Materials*, vol. 1, no. 1, 1985.

[20] C. H. Rycroft, "Voro++: A three-dimensional voronoi cell library in c++," *Chaos: An Interdisciplinary Journal of Nonlinear Science*, vol. 19, no. 4, p. 041111, 2009.

[21] A. Annamareddy and J. Eapen, "Fast anion defect recovery through superionic-type hopping displacements in uo 2 following radiation.," in *Defect & Diffusion Forum*, vol. 375, 2017.